Abdo et al., J Powder Metall Min 2017, 6:2
DOI: 10.4172/2168-9806.1000172

Journal of
Powder Metallurgy & Mining

Research Article Open Access

Density Effect of the Compacted Copper-Tungsten Shaped Charge Powder Liners on its Penetration Performance

Abdo GM* and Elshenawy T

Technical Research Centre, Cairo, Egypt

Abstract

Various copper-tungsten shaped charge compacted powder liners have been studied and discussed in this paper based on the produced liner density. Different powder compositions yield different jet characteristics when these liners are used in shaped charge penetration test. Autodyn hydrocode has been implemented to study the effect of the metal powder liner density on the produced jet characteristics. Liners have been produced by both uniaxial pressing and cold isostatic pressing techniques. Liners produced experimentally using uniaxial pressing technique exhibited density variation along the liner height, while those manufactured using cold isostatic pressing are featured by relative uniform density. The former technique with non-uniform density distribution along the liner height has shown efficiency when compared to the latter one of uniform density. The difference in the performance of the two studied liners was confirmed experimentally using static filed testing against rolled homogeneous armour (RHA) targets.

Keywords: Shaped charge; Penetration liner powder; Isostatic pressing; Uniaxial pressing

Introduction

Shaped charge jet has been used extensively due to its considerable large penetration depth into different target materials. Various liner materials have been used to manufacture shaped charge liners in research so far [1]. Zirconium, copper, silver, steel, titanium depleted uranium liners have been studied according to their jet break-up time [2-4] and effective jet length [2]. Glass liner has been tested and exhibited a larger breakup time in comparison with the traditional copper liner. Compacted powder pressing material as a shaped charge liner has been patented in 2001 by Reese et al. [5] as a shaped charge oil well perforator liner for oil and well field completion. Stinson et al. have patented the methodology for producing single phase tungsten or molybdenum liners for warhead application using hot isostatic pressing technique, after which the final liner dimensions are obtained by machining [6]. Walters et al. have tested un-sintered copper tungsten liners against steel targets at short stand-off distances using OMNI shaped charge and described the bulk spreading jet particles using flash x-ray radiograph [7]. Halliburton energy service, USA has also patented some different powder liners including tungsten, copper, lead, tantalum and molybdenum with their different loading densities to test them in the oil industry. Their invention has been implemented in the oil industry as oil well perforator to complete the well [8]. Hirsch and Mayseless discussed and analysed the characteristics of the shaped charge powder jet and its penetration capability into soft and hard targets [9]. Zhang et al. measured the jet velocity of copper-tungsten powder jet and effect of both water and air on the attenuation of its jet tip velocity [10]. Glenn used composite liner composed of copper, tungsten, graphite and tin powders for oil well perforating concrete targets [11]. All the discussed liner powder mixtures have different densities based on their initial powder composition design, which in turn yield different collapse velocities and therefore result in different jet tip velocities due to explosive metal Gurney configurations and unsteady state PER theory [12]. The density distribution was considered in the jets formed from powdered metal liners and its effect on the penetration has also been discussed analytically [13-15] and experimentally [16].

In this paper, different powder mixture liners and their density effect on the produced jet characteristics will be discussed. The expected jet characteristics of the selected powder design are obtained using Autodyn hyrdocode. Two techniques are used in the current research to manufacture copper-tungsten shaped charge compacted powder liners (as a green products non sintered liners). The uniaxial powder pressing technique and the cold-isostatic pressing processes have been implemented in our research. The density of the prepared green product liners from both techniques has been measured using helium gas pycnometer. Extensive numerical trials using Autodyn hydrocode have been performed to study the effect of liner density on the jet characteristics. The performance of the prepared liners have been assessed by the static firing of two shaped charges including powder liners manufactured differently against RHA steel targets.

Experimental Work

Material specification

Shaped charge liners have been fabricated with the designed liner composition that yield the required density. The outer casing of the shaped charges were steel 4340 of thickness 2 mm. the steel casing was manufactured from a rod of diameter 50 mm using CNC machine. A central hole of diameter 8 mm has been milled to insert the electric detonator no. 8 for the charge detonation. All the needed chemical powders for the liner have been obtained from sigma Aldrich UK, limited and these powders are used as received. The pure copper powder used as a mixture binder has an average grain size of 3 μm and a density of 8.5 g/cm^3. Tungsten acting as the main powder has small average grain size of 0.6: 1 μm in order to enhance filling the powder matrix. The binder coating material used in this mixture was

***Corresponding author:** Abdo GM, Technical Research Centre, Cairo, Egypt, Tel: +201226148750; E-mail: gm_abdo@yahoo.com

Received May 17, 2017; **Accepted** June 10, 2017; **Published** June 17, 2017

Citation: Abdo GM, Elshenawy T (2017) Density Effect of the Compacted Copper-Tungsten Shaped Charge Powder Liners on its Penetration Performance. J Powder Metall Min 6: 172. doi:10.4172/2168-9806.1000172

Tin with an average grain size lower than 45 μm and purity of 99.8%. Graphite of low percent in the powder mixture has been used as a lubricant with average grain size not exceeding 20 μm. Different types of plastic bonded explosives (PBXs) have been used for filling shaped charges; explosives could be bonded by fluorinated hydrocarbons [17], thermoset polymeric matrices [18] and thermoplastic matrices [19]. In our research, composition C-4 (RDX-C4) was used for filling the studied shaped charges [20]. RDX-C4 was prepared by mixing of 91 wt% of RDX with 9 wt% polymeric matrix [21]. It has low sensitivity, high thermal stability and detonation velocity of 8055 m/s at 1.61 g/cm^3 density [22-24]. Each shaped charge has been filled by 30 g of the C4 plastic explosive.

Liner manufacturing

Uniaxial pressing liners: The powder metallurgy (PM) technique has been used previously to manufacture these liners. It has tested before and exhibited a good penetration capability especially at short stand-off distances [7,8,25,26]. Copper-Tungsten powder liners used in this study have been manufactured using both uniaxial pressing technique and cold isostatic pressing process. The liners have small base diameter of 40 mm, a cone apex angle of 46° and uniform liner wall thickness of 1.2 mm as shown in Figure 1 for the uniaxial pressed liner. The composition of the optimized powder mixture ingredients are listed in Table 1 with the function of each ingredient. Mall average grain size with irregular particle shapes are chosen for the liner ingredients. In the uniaxial pressing technique, the powders are dried at 60°C to remove humidity and then mixed together with the designated mass ratio until the homogeneous mixture blend is obtained, after which they are pressed using Instron uniaxial hydraulic press. The applied pressure was 100 MPa using the hydraulic press at a low rate (i.e. 1 MPa per second) to avoid trapping air voids inside the liner material. The product is a brittle material in the pre-sintering state and is called 'the green product', which is tested in this state without sintering as shown in Figure 1. Figure 2 shows a schematic layout for the uniaxial pressing technique in comparison with the other cold isostatic pressing process.

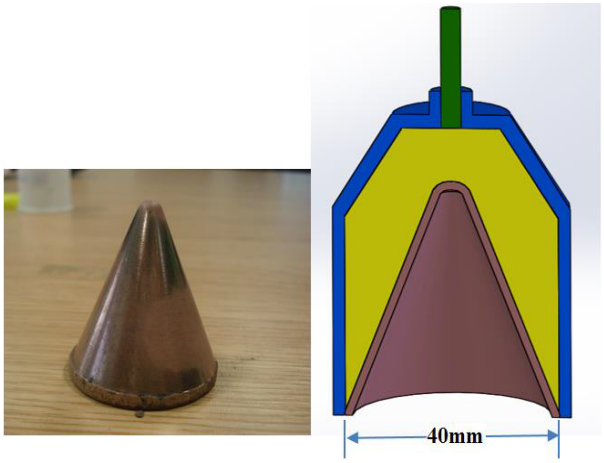

Figure 1: The produced pressed liner (left) and a sketch of the shaped charge assembly (right).

Material	Copper	Tungsten	Tin	Graphite
Mass %	43	45	11	1
Av. grain size (μm)	3	0.6:1	<45	<20
Function	Binder	Main powder	Binder coating	Lubricant

Table 1: The mass percentage of the powder liners composition.

Advantage of this techniques is the smoothness of the produced liner surface if both the punch and its die have been machined, ground and polished before pressing.

Cold isostatic pressing liners: In cold isostatic pressing (CIP) technique, the dried and mixed metal powder is placed and enclosed in a flexible polyurethane rubber mould. The assembly is then pressurized hydrostatically in a chamber usually using water. The usual values of pressures lies between 400 and 1000 MPa are normally used. The powder gets compacted and the green compact is taken out the high pressure chamber. Advantages of this technique are producing liners with relative uniform density over the entire liner height and therefore no remarkable density gradient is observed. Figure 2 shows schematic drawing of hydrostatic pressing process.

Measurement

The liner density has been measured using AccuPyc1330 helium gas pycnometer. It determines volume by measuring the pressure change of helium in a calibrated volume. The pycnometer operates on Archimedes principles of gas displacements to determine the volume. The samples are weighted on a digital scale (accuracy 0.1 mg). The analyser measures the volume of the samples, from which density can be derived. Each green product compacted powder liner is dis-integrated into tiny pieces and marked due to its position on the liner height. Several pieces are used for each liner sample. The results gave a complete picture about the effect of the pressing technique on the produced bulk density for every produced powder liner.

Experimental field testing

The explosive charges were filled into the steel casing by extrusion, and then the liners were pressed slowly against the steel casings containing explosives to avoid holding air gaps inside the explosive charge. Care should be taken during the pressing stage to avoid cracking and failure of the produced brittle green product liners. The two tested charges have been attached to the upper RHA steel layer of the test configuration as shown in Figure 3 to assess the performance of each charge in terms of its penetration depth achieved into to the RHA, which was laminated layers of RHA of total thickness 12 cm. The stand-off distance 4 cm was maintained between the charge base and the upper RHA surface. The firing of the shaped charges was done electrically using detonator no 8. The depth of penetration was measured for both charges as a measure of the compacted powder liners performance comparison.

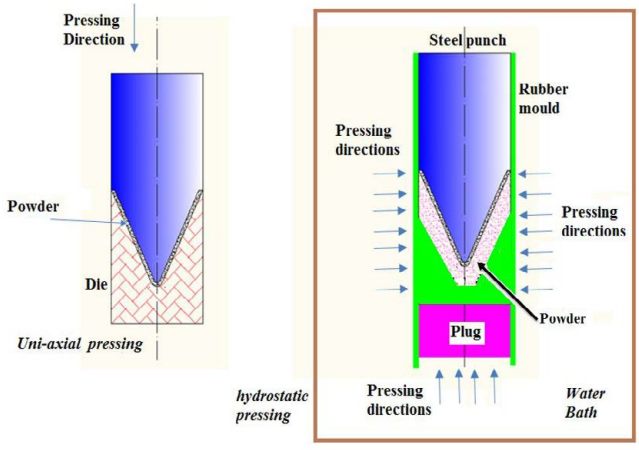

Figure 2: Sketch of the uniaxial pressing (left) and hydrostatic pressing (right).

Numerical Hydrocode

Autodyn hydrocode is used in this paper to assess the jetting characteristics of the produced jet elements considering the liner density parameter. The Autodyn shell jetting analysis algorithm is based on the analytical unsteady PER model [27], which is solved numerically using finite difference technique to calculate the jet and slug velocities, masses and the collapse velocities and deflection angles of the jet elements [28]. The jetting analysis was validated by comparing the jetting analysis results of the 90 mm shaped charge with real experimental results [29]. In this scheme, the explosive, the charge casing and the explosive materials are filled into the global Euler multi-material part [30], but the liner must be assigned as a shell element, in which the liner thickness and the solution jetting points are determined. General uniform square meshes 0.50 mm of the Euler grids were used, while a total numbers of liner jetting nodes are specified as 40 node.

The explosive required for shaped charges must have high velocity of detonation and high density to provide a high detonation pressure, which results in fast jet tip and therefore large penetration depth is achieved. The explosive material used for filling the meshes of the explosive inside the shaped charge was C4. The equation of state for the used explosive was "Jones-Wilkins-Lee" (JWL) equation, which gave the following energy equation:

$$p=A\ e\text{-}r1\ v+Be\text{-}r2\ v+C\ v\text{-}(1+\omega) \quad (1)$$

Where p is the pressure, v is the relative volume, A, B, r1, r2, C and ω are constants. The values of these constants for many common explosives have been determined from dynamic experiments. The values of these constants should be considered as a set of interdependent parameters. The input data to AUTODYN-2D for the explosive material are listed in Table 2.

The material used for the charge case was steel 4340. The equation of state for the steel is shock EOS, while its strength model was Johnson-Cook. This constitutive model aims to model the strength behavior of materials subjected to large strains, high strain-rates and high temperatures [30]. The model defines the dynamic yield stress Y [31] as:

$$\sigma=(A+B\varepsilon^{n})(1+C\ln[\varepsilon^{*}])(1-T_{H}^{m}) \quad (2)$$

Where σ is the dynamic flow stress, ε is the effective plastic strain, A is the yield strength, B is the hardening constant, n is the hardening exponent, C is the strain-rate constant and m is the thermal exponent constant. ε^{*} is the normalized effective plastic strain-rate (i.e. the applied true strain-rate divided by the reference strain-rate). TH is the homologous temperature. The five material constants are A, B, C, n and m. The expression in the first set of brackets gives the stress as a function of strain when ε* equal to 1.0 sec^{-1} and TH=0 for laboratory experiments at room temperature. The expressions in the second and third sets of brackets represent the effects of strain-rate and temperature, respectively. The constants in these expressions determined by means of material tests over a range of temperatures and strain-rates. The input data to Autodyn for the case material are listed in Table 3.

The material modelling of the copper tungsten powder is more complicated than that of the pure material because it required some dynamic material testing to conclude its mechanical properties such as shock Equation of state. Alternative method has been implemented within this research, which had been used successfully by Yingbin and Zhaowu [26]. The theory of mixture rule simply calculates a certain mixture parameters by formulating its parameters with component percent fractions. The selected equation of state of the liner material is the linear EOS. The present form of this equation considering the initial elastic behaviour expressed by an approximation to Hooke's Law which can be written as:

$$p=K \quad (3)$$

Where p is the pressure, μ is the compressibility and equals (ρ/ρ_0)-1, K is the bulk modulus, ρ_0 is the reference density and ρ is the current density. The input data to AUTODYN-2D for the calculated liners are shown in Table 4.

Figure 3: Test setup and the experimental test configuration.

Parameter	Value
Density (g/cm³)	1.61
Parameter A (KPa)	6.0977×10^{8}
Parameter B (KPa)	1.295×10^{7}
Parameter r_1	4.5
Parameter r_2	1.5
C-J detonation velocity (m/s)	8055
C-J energy/unit volume (kJ/m³)	9×10^{6}
C-J pressure (kPa)	2.8×10^{7}
Parameter ω	0.25

Table 2: Input data to Autodyn for C4 explosive charge.

Reference density (g/cm³)	7.83
Tensile strength (MPa)	744
A (MPa)	792
B (MPa)	510
n (non)	0.26
C (non)	0.014
m (non)	1.03
Gruneisen coefficient	1.93
Parameter C_1 (m/s)	4569
Parameter S_1 (non)	1.4
Ref. temperature (K)	300

Table 3: Input data to the code for the charge casing material [30].

Material	Tungsten (%)	Copper (%)	Tin (%)	Graphite (%)	Density (g/cm³)	Bulk mod. (MPa)
Function	Main powder	Binder	Binder coating	Lubricant		
A	31	57	11	1	10.38	1.82×10^{5}
B	52	37	10	1	12.30	2.19×10^{5}
C	72	19	8	1	14.16	2.54×10^{5}
D	90	5	4	1	15.90	2.88×10^{5}
E	96	2	1	1	16.53	3.01×10^{5}

Table 4: The designed powder mixtures for the numerical study.

Results

Density effect on the produced jet characteristics

According to Gurney formula for different explosive-metal configurations, various jet characteristics have been obtained because of the effect of the explosive-metal mass ratios. Table 5 lists the jetting output summary results for different densities liners obtained from Autodyn numerical work. It can be simply concluded that the liner densities has shown a direct influence on the produced jet velocities. Theoretically the most efficient jet tip velocity is expected to be of the lowest density of 10.38 g/cm^3, that has the largest kinetic energy of 44.3 kJ, but other parameters of direct importance, which cannot be neglected, which are the breakup time and the effective jet length that must also be considered. Besides, the binder coating percentages lower than 10% have a negative effect on the cohesiveness of the produced green product liners. Therefore, the range of the liner density that will be prepared experimentally is from 10.38 to 12.30 g/cm^3. Thus, the real liner preparations and their testing include both liners; uniaxial pressing and isostatic liners for penetration performance comparison within the selected density range.

Liner density measurement

The density measurement of the liners was carried out using AccuPyc1330 helium gas Pycnometer. The liners were disintegrated and cut down at different distances from its apex, and then the density of every part is determined independently using a single density measurement trial. Figure 4 demonstrates the relation between density and the distance from the apex for both numerical and measured experimental measurements for both cold isostatic liner and uniaxial pressed powder liners. Due to the fact of the forces distribution over the inclined cone part of the liner and the non-uniform stresses distribution, non-regular density profile has been obtained as shown in the uniaxial pressed powder liner. The apex region has more stress that result in squeezing the powder between both upper punch and lower die, which results in this density gradient. However, general attitude between the numerical and the real density is observed as shown in Figure 4. On the other hand, the cold isostatic powder liner exhibited relative homogeneous density in comparison with previous one.

Numerical simulation for the density profile of the liner produced by powder compaction using uniaxial pressing technique at different times have been demonstrated on Figure 5.

Penetration performance of the two studied liners

The standard jetting analysis has been conducted on the two liners considering the density obtained from the real measurements. Figure 6 shows the jet velocity-cumulative jet mass fingerprints for the studied two liners; uniaxial pressed liner and isostatic pressed one obtained by jetting analysis. The two liners have nearly the same pattern, but slight velocity difference can be observed between them. The figure shows slight increase in the jet tip velocity of the uniaxial pressed liner due to its lower density at the jet tip section, but their jet tails have very close values of 3500 and 3583 m/s. The difference between their jet lengths (as listed in Table 6) shows that the uniaxial pressed liner has about 7 mm excess in the jet length more than the other isostatic one. This difference is confirmed by the performance penetration depth of the two shaped charges including both manufactured liners. The two penetration tests have been conducted in the same way at the same

Liner	Liner average bulk density (g/cm^3)	Liner Geometry		Output					
		Thick. (mm)	Mass (g)	Jet tip vel.V_j (m/s)	Jet tail velocity V_t (m/s)	Jet KE (kJ)	Break-up time t_b(μs)	Average jet radius (mm)	Jet length (V_j-V_t) t_b (mm)
A	10.38	1.2	36.7	5977	3750	44.3	32.5	1.50	72.38
B	12.30	1.2	42.0	5610	3690	43.7	32.8	1.56	62.98
C	14.16	1.2	42.96	5430	3662	42.0	30.2	1.43	53.39
D	15.90	1.2	48.3	5270	3460	41.0	29.4	1.40	53.21
E	16.53	1.2	52.1	4980	3251	39.5	28.7	1.36	49.62

Table 5: The jetting output results for different densities linear.

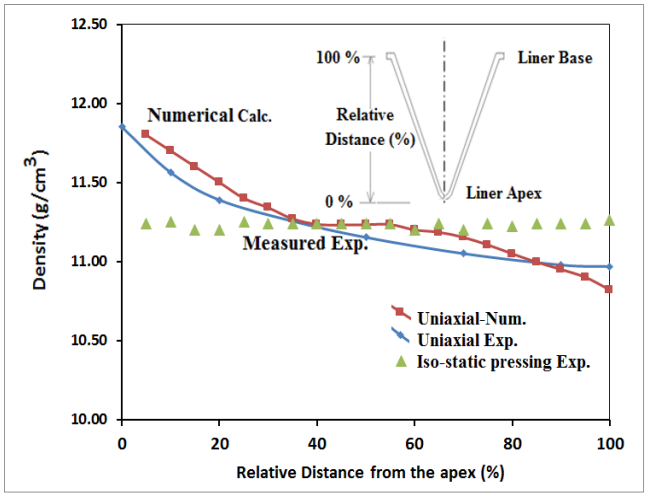

Figure 4: The measured and calculated densities at different distances from the liner apex.

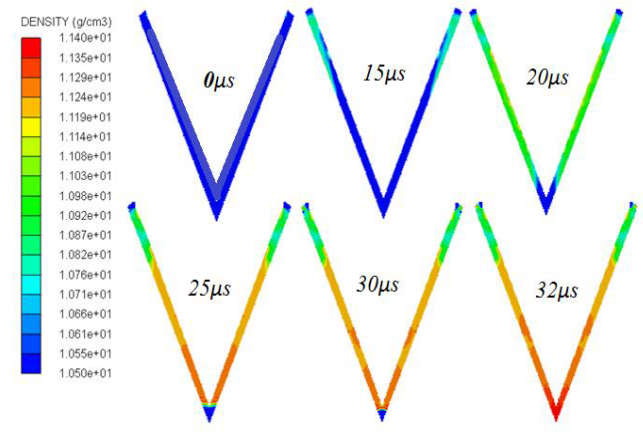

Figure 5: Density profile at different times from the begining of powder pressing for the uniaxial pressed powder liner.

Liner type	Liner density (g/cm³)	Liner Geometry		Output					
		Thick. (mm)	Mass (g)	Jet tip vel. V_j (m/s)	Jet tail velocity V_t (m/s)	Jet KE (kJ)	Break-up time t_b (µs)	Average jet radius (mm)	Jet length $(V_j-V_t)t_b$ (mm)
Uniaxial liner	11.85: 10.65	1.2	32.9	6272	3500	45.2	31.6	1.50	87.59
Isostatic liner	Average11.25	1.2	33.5	6122	3583	44.8	31.8	1.51	80.74

Table 6: The performance of the uniaxial and isostatic liner based on real density measurements.

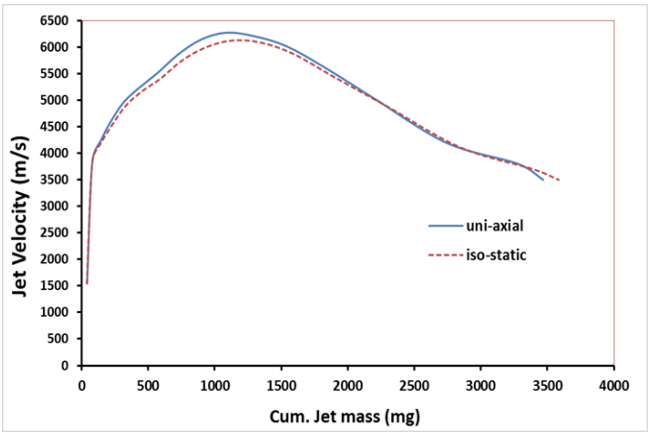

Figure 6: The jet velocity-cumulative jet mass for the studied two liners; uniaxial pressed liner and isostatic pressed one.

Figure 7: The shaped charge penetration testing against RHA target; right: using uniaxial pressed liner; left: hydrostatic pressed liner.

specified stand-off distances using the RHA targets. The penetration effect of the liner produced by uniaxial pressing showed enhanced penetration in comparison with other uniform density liner produced by isostatic liner as shown in Figure 7. The obtained penetration depths were 10.5 cm and 9.7 cm into RHA for uniaxial and isostatic pressing liners respectively (i.e. 8% excess).

Conclusions

Unlike powder liners produced by cold isostatic pressing technique, the powder liner produced using uniaxial pressing technique exhibited non-uniform density distribution along the liner height. It has been shown that density of the liner material has significant effect on the produced jet characteristics. The liner produced by uniaxial pressing, which exhibited non-uniform density distribution, has larger effective jet length than that produced with cold isostatic liner. Therefore, it has achieved penetration depth into RHA target material larger than that achieved with cold isostatic liner with uniform density.

References

1. Buc SM (1991) Liner Materials: Resources, Processes, Properties, Costs, and Applications.
2. Bourne B, Cowan KG, Curtis JP (2001) Interlaken, Switzerland.
3. Elshenawy T, Li QM (2013) Breakup Time of Zirconium Shaped Charge Jet Propellants, Explosives, Pyrotechnics 38: 703-708.
4. Elshenawy T (2015) Determination of the Velocity Difference between Jet Fragments for a Range of Copper Liners with Different Small Grain Sizes Propellants, Explosives, Pyrotechnics.
5. Reese JW, Hetz A (2001) Coated metal particles to enhance oil field shaped charge performance Google Patents.
6. Stinson JS (1996) Method for producing high density refractory metal warhead liners from single phase materials.
7. Walters W, Summers R, Leidel D (2001) A study of jets from unsintered powder metal lined non precision small caliber shaped charge.
8. Leidel DJ, Lawson JP (2001) High performance powder metal mixtures for shaped charge liners USA.
9. Hirsch E, Mayseless M (2010) Penetration of Porous Jets. J Applied Mechanics 77.
10. Zhang X, Wu C, Huang F (2010) Penetration of shaped charge jets with tungsten-copper and copper liners at the same explosive-to-liner mass ratio into water. Shock Waves 20: 263-267.
11. Glenn LA (2001) Pressure enhanced penetration with shaped charge perforators USA.
12. Walters P, Zukas J (1989) Fundamentals of shaped charge. Wiley Interscience Publication New York, USA.
13. Mostert KD, Wa FJ (2004) Analytical model predicting the penetration behaviour of a jet with a time-varying density profilelocity density profiles. South Africa.
14. Milton FM, Wa KD, FJM (2005) An analytical penetration model for jets with varying mass density profiles in 22nd International symposium on Ballistics.
15. Grove B (2007) Shaped Charge Jet Velocity and Density Profiles in 23rd International Symposium on Ballistics Spain.
16. Elshenawy TA, Elbeih, LI QM (2016) A Modified Penetration Model for Copper-Tungsten Shaped Charge Jets with Non-uniform Density Distribution. Cent Eur J Energ Mater13: 927-943.
17. Elbeih A (2013) Study of Plastic Explosives Based on Attractive Cyclic Nitramines. Part II Detonation Characteristics of Explosives with Polyfluorinated Binders, Propellants, Explosives Pyrotech 38: 238-243.
18. Elbeih A, Wafy TZ, Elshenawy T (2017) Performance and Detonation Characteristics of Polyurethane Matrix Bonded Attractive Nitramines.
19. Yan QL (2013) The influence of the Semtex matrix on the thermal behavior and decomposition kinetics of cyclic nitramines. CE J Energetic Materials 10: 509-528.
20. Elbeih A (2012) Effect of different polymeric matrices on the sensitivity and performance of interesting cyclic nitramines. CE J Energetic Materials 9: 131-138.
21. Elbeih A (2012) Detonation characteristics of plastic explosives based on attractive nitramines with polyisobutylene and poly (methyl methacrylate) binders. J Energetic Materials 30: 358-371.
22. Elbeih AS, Zeman, J Pachman (2013) Effect of polar plasticizers on the characteristics of selected cyclic nitramines. CE J Energetic Materials 10.
23. Pelikán V (2014) Concerning The Shock Sensitivity Of Cyclic Nitramines Incorporated Into A Polyisobutylene. Matrix CE J Energetic Materials 11: 219-235.
24. Yan QL (2017) Non-isothermal analysis of C4 bonded explosives containing different cyclic nitramines. Thermochimica Acta 556: 6-12.
25. Zygmunt B, Wilk Z (2008) Formation of jets by shaped charges with metal powder liners. Propellants, Explosives, Pyrotechnics 33: 482-487.

26. Yingbin L, Zhaowu S (2010) Numerical simulation on formation and penetration target of powder metal shaped charge jet. In Computer Application and System Modeling (ICCASM).

27. Pugh EM, Eichelberger JR, Rostoker N (1952) Theory of jet formation by charged with lined conical cavities. J Applied Physics 23: 532-536.

28. Elshenawy T, Li Q (2013) Influences of target strength and confinement on the penetration depth of an oil well perforator. Int. J of Impact Engineering 54: 130-137.

29. Malcolm S (1997) Autodyn jetting tutourial R. 3.0, Century Dynamics: USA.

30. Team A (1997) Autodyn Theory Manual Century Dynamics CA.

31. Johnson G, Cook W (1983) A Constitutive Model and Data for Metals Subjected to Large Strains, High Strain Rates and High Temperatures.